EAI Endorsed Transactions
on AI and Robotics
Research Article EAI.EU

An adaptive traditional Chinese herbal medicine image recognition model via ED-HLOA-optimized DenseNet201

Peiyang Wei[1],[2,3], Rundong Zou[1], Guangtong Dong[4*], Xun Deng5, Wen Qin[6], Jianhong Gan[1], Qifeng Su[7,8*] and Zhibin Li[1,5]

[1]School of Software Engineering, Chengdu University of Information Technology, Chengdu, 610225, China
[2]School of Computer Science and Technology, Chongqing University of Posts and Telecommunications, Chongqing 400065, China
[3]Automatic Software Generation & Intelligence Service Key Laboratory of Sichuan Province, Chengdu 610225, China
[4]School of Traditional Chinese Medicine, Beijing University of Chinese Medicine, Beijing 100029, China
[5]Xinjiang Technical Institute of Physics &Chemistry, Chinese Academy of Sciences, Urumqi 830011, China
[6]School of Computer Science, Sichuan Normal University, Chengdu 610101, China
[7]School of Big Data and Artificial Intelligence, Chengdu Technological University, Chengdu 611730, China
[8]College of Mathematics and System Sciences, Xinjiang University, Urumqi 830017, China

Abstract

Research shows that ginseng, fritillaria cirrhosa and other Chinese herbal medicines (CHM) and their active components can fight tumors via immune regulation, apoptosis induction, and signaling pathway modulation. Thus, deep learning-based for authentic Chinese herbal medicine identification and classification is gaining more attention. Although convolutional neural network (CNN)-based image recognition models have made progress in CHM recognition, they often face limitations such as simple structures, fixed parameters, and a singular optimization approach, primarily relying on learning rate adjustments, which impede achieving the high accuracy required for image recognition of CHM. To address this issue, this study proposes an elite differential mutation-based horned lizard optimization algorithm (ED-HLOA) and applies it to optimize a DenseNet201-based recognition model for CHM. It enables adaptive adjustments of the learning rate and compression factor for DenseNet201. Empirical studies on the dataset collected from practical application demonstrates that the ED-HLOA-optimized DenseNet201 model achieves high accuracy in CHM image classification, verifying the effectiveness of the algorithm. Compared with several state-of-the-art optimization algorithms, ED-HLOA performs well on both the training and verification sets, effectively avoiding overfitting.

Keywords: Chinese Herbal Medicine, tumors, Neural Network, Self-Adaptive Model, Image Recognition, Horned Lizard Optimization Algorithm.

Received on 17 June 2025, accepted on 30 June 2025, published on 21 July 2025

doi: 10.4108/airo.9563

*Corresponding author. Email: 1007809206@qq.com, sqfeng1@cdtu.edu.cn

1. Introduction

As a treasure of Chinese traditional culture, traditional Chinese medicine (TCM) shows unique advantages and remarkable curative effects in complex diseases such as cancers, cardiovascular diseases, and autoimmune disorders[1-4]. In recent years, an increasing number of studies demonstrate that Chinese Herbal Medicine (CHM) and their active components exhibit significant inhibitory effects in the clinical treatment of tumors. Wu et al. prove that ginsenoside Rh2 can inhibit the proliferation and induce apoptosis of glioma cells by upregulating the expression of miR-128 [5]. Tan et al. reveal that ginsenoside F2 derived from ginseng effectively regulates the occurrence and development of hepatocellular carcinoma by inhibiting the STAT3 signaling pathway [6]. Li et al. summarize and

propose the application of CHM in the treatment of non-small cell lung cancer, indicating that CHM and their active components play a positive role in immune regulation and anti-tumor processes [7]. And wang et al. indicate that CHM can inhibit the occurrence and development of cancer by regulating tumor metabolic reprogramming processes (such as glycolysis and lipid metabolism), demonstrating the unique advantages of multi-target and multi-pathway anti-cancer effects [8].

The identification and classification of CHM provide fundamental resources for the treatment of related tumor diseases, yet remaining challenges in recognizing complex features [9-10]. Traditional recognition methods primarily rely on the expertise of specialists, a process that is both time-consuming and labor-intensive, and are influenced by subjective factors. These limitations hinder the ability to meet the demands of modern and large-scale applications, thus hindering the promotion and development of TCM [9-10]. In recent years, the rapid development of deep learning technologies, particularly convolutional neural networks (CNNs), has provided new ideas and methods to address this issue [11-15]. Image recognition technology has made breakthroughs in many fields, such as real-time abnormal behavior detection and target tracking in security monitoring [16]; Improve vehicle environment perception and decision-making ability in the field of autonomous driving [17-18]; Improve the accuracy and efficiency of product quality control in industrial vision inspection applications [19]; Assist in the early detection and diagnosis of diseases in the field of medical diagnosis [20-21]. Moreover, deep learning has also achieved remarkable results in areas such as intelligent recommendation, agricultural disease identification, and graph-based image classification [22-24].

In image classification tasks, CNN can automatically learn important features in images and map them to corresponding categories, thus achieving high-precision classification. However, the traditional CNN model has some significant shortcomings in application. Firstly, as the depth of the network increases, the training process may encounter issues of vanishing or exploding gradients, making it difficult for the model to train effectively. Secondly, deeper network architectures typically require substantial computational resources and memory, which reduces the efficiency of both training and inference. Furthermore, the traditional structure of CNNs often leads to parameter redundancy, with an excess of parameters potentially causing overfitting, especially evident when training on small datasets. To address these challenges, many new network architectures have emerged. For example, He et al. proposes that ResNet effectively alleviates the problem of gradient disappearance in deep networks by introducing skip connections [25] and improves the feasibility of training deep networks. Although ResNet can improve the training effect, there is still room for improvement in feature reuse and computational efficiency. GoogLeNet(Inception)[26] improved the representation of the model by using convolution and pooling kernels of different sizes to capture features at different scales, but the network design and adjustment are more complex. Huang et al. proposes an improved network architecture DenseNet [27], which successfully solved some key problems in traditional networks by introducing a dense connection mechanism. In addition, Chen et al. demonstrated that it is possible to enhance the representational capacity of deep neural networks with minimal parameter increase, providing a useful perspective for optimizing model efficiency in practical applications [28].

Currently, image recognition technology based on deep neural networks has achieved significant advancements in the field of CHM image recognition. Research indicates that deep learning models can attain recognition accuracies exceeding 90% in the image recognition of CHMs such as Hawthorn and Spinelli. Even when faced with CHMs like Fritillaria that share similar colors and shapes, these models continue to demonstrate satisfactory recognition accuracy. This progress is largely attributed to the widespread application of CNNs [29-30], along with the incorporation of intelligent optimization algorithms such as tribe evolution, black widow, and egret swarm optimization, which further enhance training stability and parameter tuning [31-33]. This deep learning approach not only enhances the recognition rates of CHMs but also provides new ideas and methods for quality control and intelligent comprehensive management of CHMs.

Although the currently widely utilized CNN models have achieved significant advancements in the field of CHM image recognition, these models tend to be relatively simplistic, characterized by fixed parameters and an optimization process limited to learning rate adjustments. Consequently, they struggle to meet the high precision requirements essential for CHM image recognition. The manual tuning of hyperparameters often relies on empirical grid search methods, which can prolong the optimization process significantly. Additionally, suboptimal grid spacing may adversely affect model accuracy. Studies have shown that employing evolutionary computation algorithms for the selection and optimization of hyperparameters can substantially reduce the workload associated with parameter adjustments during the training of deep neural networks, while effectively enhancing exploration efficiency [34-36]. Bajaj et al. utilize the optimization capability of genetic algorithms to handle complex error functions, achieving more effective parameter estimation [37]; Based on the particle swarm optimization algorithm (PSO), Wang et al. proposed a new method for calculating particle differences and updating velocity mechanisms, which reduces the parameter search space [38]; Kong et al. propose egret swarm algorithm (ESOA) to find the best solution based on egret group cooperation [39].

To meet the urgent demand for the accurate identification and classification of Chinese herbal materials from medical research institutions, Chinese medicine enterprises, pharmaceutical manufacturing companies, Chinese medicine schools, and individuals interested in TCM, this paper combines improved convolutional neural networks with optimization algorithms. The aim is to develop a CHM recognition model characterized by high predictive accuracy and adaptive hyperparameter tuning. The primary concept involves integrating elite differential mutation into the lizard optimization algorithm, using the optimized algorithm to

learn the hyperparameters of a CHM recognition model based on DenseNet201. This approach enables the adaptive tuning of both the learning rate and compression factor, thereby enhancing the accuracy of CHM recognition. The main contributions of this work include:

a) Collection and sorting of datasets from five categories on CHM in real applications, and preprocessing operations including dimension reduction, clipping and conversion were performed on these pictures for generalization; and

b) A novel Horned lizard optimization algorithm (ED-HLOA), based on elite differential variation and applied to the CHM recognition model utilizing DenseNet201; and

c) Experimental analysis of Chinese herbal medicine recognition model based on ED-HLOA.

Experimental validation on homemade datasets. The authors have not seen similar efforts in previous studies.

Section 2 reviews the previous work. Section 3 introduces the Chinese herbal medicine recognition model based on ED-HLOA. Section 4 shows the experimental results. Finally, Section 5 summarizes this paper.

2. Preliminaries

2.1. DenseNet201

In DenseNet [27], each layer is connected to all preceding layers. This dense connectivity not only effectively alleviates the vanishing gradient problem but also significantly enhances the efficiency of feature reuse. The dense connectivity mechanism ensures that information is thoroughly propagated throughout the network, thereby reducing the computational resources required for training deep networks and effectively minimizing parameter redundancy. Furthermore, DenseNet, with its efficient feature propagation mechanism, can effectively avoid overfitting when handling smaller datasets, demonstrating outstanding performance across multiple tasks. To optimize the performance of the CHM image classification task, this study selects DenseNet201 as the backbone network. The structural diagram of DenseNet201 is shown in Fig. 1.

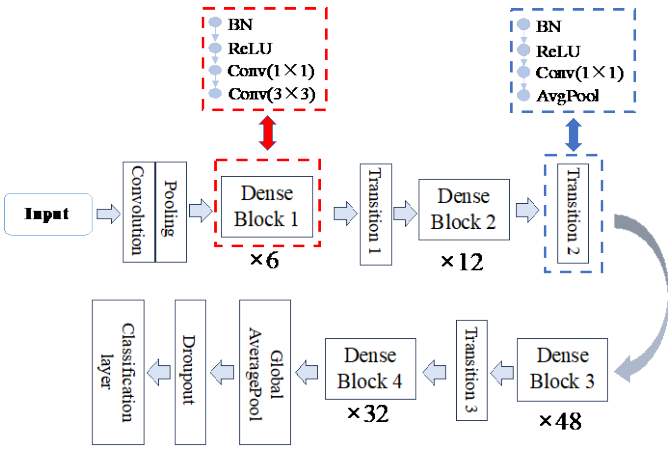

Figure 1. The structural diagram of DenseNet201

2.2. Horned lizard optimization algorithm

Peraza-Vázquez et al. propose a novel bio-inspired optimization algorithm i.e., Horned Lizard Optimization Algorithm (HLOA) [40]. It comprehensively simulates various defensive behaviors of the horned lizard, including camouflage, color change, blood-squirting, and fleeing. This algorithm mimics the horned lizard's adaptation to its environment by changing its color and adjusting skin brightness to control solar heat gain, while also considering the impact of the rate of α-melanocyte-stimulating hormone (α-MSH) on color change.

The HLOA develops both global and local search capabilities for optimizing the learning rate and dropout rate of DenseNet201. However, once in the development phase, the HLOA has a high demand for local search capability; poor local search performance can lead the algorithm to become trapped in local optima. The HLOA integrates five defensive strategies, where the camouflage strategy relies on environmental conditions, the color change strategy can easily cause solutions to become stuck in local minima, and the blood-squirting strategy, while capable of making large jumps, can also lead to passive situations. To proactively predict the next optimal position, this study employs elite differential mutation [41-42] to explore target locations, thereby actively adjusting parameters to escape local optima. The specific implementation plan is discussed in Sections 3 and 4.

3. Methods

In this section, a CHM recognition model based on ED-HLOA is proposed, which realizes the adaptive adjustment of DenseNet201 learning rate and compression factor.

3.1. Data collection and processing

This study constructed a CHM dataset, which includes five categories: Peppermint, Fritillaria cirrhosa, Honeysuckle, Ophiopogon, and Ginseng, totaling 10,100 images. The dataset primarily is provided by a collaborating traditional Chinese medicine university. To enhance the diversity and robustness of the dataset, various data augmentation operations were performed on the data from the five categories, including rotation, scaling, cropping, and pixel normalization. These preprocessing steps ultimately resulted in the enhanced dataset used for CHM image classification in this study.

Image Acquisition. As a result of our project collaboration with a certain traditional Chinese medicine university, we obtained over 200 categories of images, totaling more than 2,000 pictures of CHM, providing valuable and diverse data resources for our research. Based on these images, we performed precise annotation and classification for each category of herbs, ultimately constructing a dataset that encompasses 259 categories and over 3,500 original images of CHM. This dataset covers

various growth stages, angles, and lighting conditions of the herbs, providing rich material for subsequent research and applications.

Image Enhancement. To enhance the model's learning capabilities and improve training efficiency, five representative categories of herbal medicine are selected from the entire herbal image dataset for image augmentation. Each category contains 45 original images, and after the image augmentation process, the number of images in each category is expanded to 2,020, resulting in a total of 10,100 augmented images across the five categories. The image augmentation process includes three main steps: First, the images undergo rotation, rotating them by 90 degrees, 180 degrees, and 270 degrees to increase the sample diversity from different perspectives. Second, cropping operations are performed, with the cropping ratio set between 60% and 90%, randomly selecting different regions from the original images while preserving the key features of the herbs. Finally, the cropped images are rotated again to further enhance the diversity and complexity of the images.

These enhancement operations are designed to alleviate the overfitting problem by increasing the diversity of data and making the model more robust. In the processed image samples, the core features of the medicine are retained, and the model's recognition ability under different viewing angles and deformation conditions is enhanced. Fig. 2 shows the specific effects of the above image enhancement operations.

Image Processing. In this study, the significant differences in the original image sizes present an important challenge for the model when processing image data. To address this issue, all images undergo uniform resizing and are standardized to 224x224 pixels. This adjustment step not only ensures the consistency of the input data dimensions but also significantly reduces the model's memory usage and computational requirements. By scaling all images to a uniform size, we enhance the efficiency of data processing and improve the model's stability and reliability during the training process. This standardization process helps to simplify the data input workflow, ensuring that the model can efficiently utilize the image information, thereby increasing overall performance and training effectiveness.

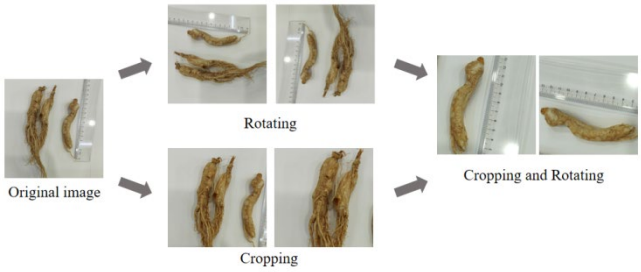

Figure 2. An example of the Ginseng rotation and cutting process.

Data Set Processing. Considering the wide variety of images in the data set, in order to concentrate the learning ability of the model and improve the training efficiency, we selected 5 representative categories of medicinal materials from all the categories for focused training and defined the mapping relationship between medicinal materials and digital labels. The data set is divided into the training set and the test set according to the ratio of 80% and 20%. In addition, to evaluate and tune the performance of the model during the training process, 10% of the 80% training data is allocated to validation sets. This ensures that the model can be effectively validated and adjusted during training, while an independent test set is used to assess the model's ability to generalize to new data. The basic information on the five medicinal materials is shown in Table 1.

Table 1. CHM Datasets

medicinal materials	Total images number	label
Peppermint	2020	0
Fritillaria cirrhosa	2020	1
Honeysuckle	2020	2
Ophiopogon	2020	3
Ginseng	2020	4

3.2. Elite differential mutation-based horned lizard optimization algorithm

Although the DenseNet201 model shows strong performance, its effectiveness is still affected by hyperparameters such as learning rate and compression factor. The learning rate controls how quickly the model adjusts its weights during training; high learning rates can lead to unstable updates, while low learning rates can lead to slower convergence or stagnation. The compression factor determines the reduction in the number of feature mappings between dense blocks, affecting the capacity and computational efficiency of the model. Two hyperparameters must be carefully adjusted to balance accuracy and resource consumption. In this section, a new adaptive hyperparameter optimization algorithm ED-HLOA is designed for DenseNet201. The overall framework of our proposed model is shown in Fig 3.

The Horned Lizard Optimization Algorithm (HLOA) fully simulates various defensive behaviors of horned lizards to adjust hyperparameters, including concealing skin color changes, spurting blood and fleeing. The detailed process for each strategy is described below.

(a) Crypsis behavior Strategy is that organisms blend into the surrounding environment by imitating environmental characteristics, making it difficult for predators or prey to find them. This behavior is modeled as a position update mechanism in the optimization algorithm, which uses the current optimal position x _best (t) and the transformation term based on color theory [29] to update the individual position, as shown in (1):

$$\vec{x}_i(t+1) = \vec{x}_{best}(t) + \left(\partial - \frac{\partial \cdot t}{Max_iter}\right)\left[c_1\left(sin(\vec{x}_{r1}(t)) - cos(\vec{x}_{r2}(t))\right) - (-1)^{\sigma} c_2\left(cos(\vec{x}_{r3}(t)) - sin(\vec{x}_{r4}(t))\right)\right] \quad (1)$$

where $\overrightarrow{x_i}(t+1)$ represents the position of the new individual in the population space at generation t+1; $\overrightarrow{x_{best}}(t)$ is the best individual from generation t; r_1, r_2, r_3, and r_4 are random integers generated between 1 and the maximum population size; $\overrightarrow{x_{r_1}}(t)$, $\overrightarrow{x_{r_2}}(t)$, $\overrightarrow{x_{r_3}}(t)$ and $\overrightarrow{x_{r_4}}(t)$ are the selected individuals from the population corresponding to r_1, r_2, r_3, and r_4 ; Max_iter denotes the maximum number of iterations, while σ and ∂ are constants; c_1 and c_2 are random numbers extracted from a normalized palette.

(b) Skin darkening or lightening Strategy can make the skin of horned lizards lighter or lightening [1] Specifically, reflecting lighter skin effectively repels heat, while darker skin increases heat absorption by absorbing more light energy The strategy of the horned lizard's skin color change can be represented by (2) and (3) as follows:

$$\vec{x}_{worst}(t) = \vec{x}_{best}(t) + \frac{1}{2} Light_1\, sin\left(\vec{x}_{r1}(t) - \vec{x}_{r2}(t)\right) - (-1)^{\sigma} \frac{1}{2} Light_2\, sin\left(\vec{x}_{r3}(t) - \vec{x}_{r4}(t)\right); \quad (2)$$

$$\vec{x}_{worst}(t) = \vec{x}_{best}(t) + \frac{1}{2} Dark_1\, sin\left(\vec{x}_{r1}(t) - \vec{x}_{r2}(t)\right) - (-1)^{\sigma} \frac{1}{2} Dark_2\, sin\left(\vec{x}_{r3}(t) - \vec{x}_{r4}(t)\right) \quad (3)$$

where, (2) describes strategies for lightening skin, while (3) describes strategies for darkening skin.

(c) Blood-squirting strategy defends enemies by squirting blood from the eyes, a defense mechanism modeling process that combines horizontal and vertical velocity components, as well as the current optimal position and individual position. Finally, the position update of an individual can be represented by the following:

$$\vec{x}_i(t+1) = \left[v_0 cos\left(a \frac{t}{Max_iter} + \varepsilon\right)\right]\vec{x}_{best}(t) + \left[v_0 sin\left(a - \frac{t}{Max_iter} - g\right) + \varepsilon\right]\vec{x}_i(t) \quad (4)$$

where $\overrightarrow{x_i}(t+1)$ represents the position of the new individual in the population space at generation t+1; $\overrightarrow{x_{best}}(t)$ is the best individual from generation t; Max_iter denotes the maximum number of iterations.

(d) Strategy can move randomly and quickly in the environment to avoid predators, and this avoidance strategy is modeled mathematically as follows:

$$\vec{x}_i(t+1) = \vec{x}_{best}(t) + walk\left(\frac{1}{2} - \varepsilon\right)\vec{x}_i(t) \quad (5)$$

where $\overrightarrow{x_i}(t+1)$ represents the position of the new individual in the population space at generation t+1; $\overrightarrow{x_{best}}(t)$ is the best individual from generation t; walk is a random number generated between -1 and 1.

(e) α-melanophore stimulating hormone (α-MSH) rate strategy is about the effect of temperature on α-MSH.

$$\vec{x}_i(t) = \vec{x}_{best}(t) + \frac{1}{2}[\vec{x}_{r1}(t) - (-1)^{\sigma}\vec{x}_{r2}(t)] \quad (6)$$

where $\overrightarrow{x_{best}}(t)$ is the best individual from generation t; r_1 and r_2, are random integers generated between 1 and the maximum population size; $\overrightarrow{x_{r_1}}(t)$ and $\overrightarrow{x_{r_2}}(t)$ are the selected individuals from the population corresponding to r_1 and r_2.

HLOA possesses both global and local search capabilities for optimizing the learning rate and dropout rate of DenseNet201. However, once it enters the development phase, HLOA has a high demand for local search capability, and poor local search performance can lead the algorithm to become trapped in local optima. HLOA combines five defense strategies, where the concealment strategy relies on environmental conditions, the skin color change strategy can easily lead to solutions being trapped in local minima, and the blood-spraying strategy, while capable of making large jumps, can also result in passive situations. To proactively predict the next best position, this study employs elite differential mutation to explore target locations, thereby actively adjusting parameters to escape local optima.

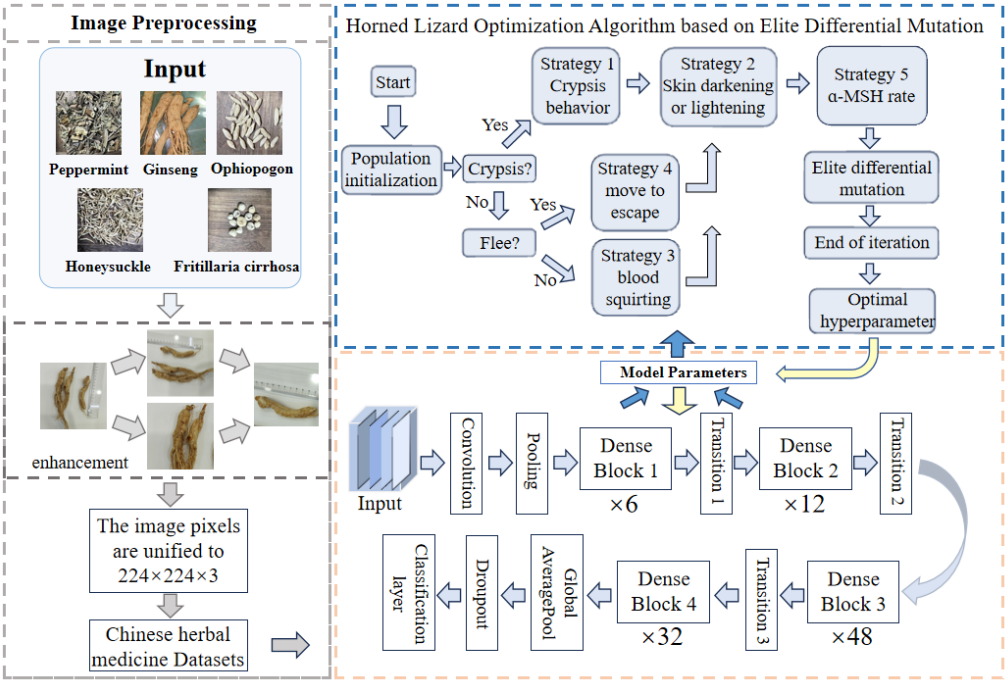

Figure 3. Overall framework of ED-HLOA

The traditional differential evolution algorithm relies on randomly selected individuals for mutation, while elite differential mutation utilizes the best individual X_{best} from the current generation. By guiding the search direction of individuals toward the region of the global optimum, it enhances the convergence speed of the algorithm and the accuracy of the solutions. The specific execution process is as follows:

Assuming the population size is N, that is, $P = \{X_1, X_2, \dots, X_N\}$, each individual is a D-dimensional vector representing a solution to the problem. The formula for generating new individuals using elite differential mutation is as follows:

$$X_{new} = X_i + F \cdot (X_{best} - X_i) + F \cdot (X_{r1} - X_{r2}) \quad (7)$$

where X_i is the optimal individual of the current iteration; X_{best} is the global optimal individual, and F is the scaling factor; X_{r1} and X_{r2} are two different individuals randomly selected from the population. The newly generated individual X_{new} will update the global optimal solution by the following:

$$X_{best} = \begin{cases} X_{new}, f(x_{new}) = min\big(f(X_{new}), f(X_i), f(X_{best})\big) \\ X_i, f(X_i) = min\big(f(X_{new}), f(X_i), f(X_{best})\big) \\ X_{best}, f(X_{best}) = min\big(f(X_{new}), f(X_i), f(X_{best})\big) \end{cases} \quad (8)$$

Through this strategy, elite differential mutation can effectively guide individuals toward the global optimum, significantly enhancing the algorithm's global search capability, accelerating the convergence process, and reducing the number of iterations required to find the optimal solution, thereby improving optimization efficiency.

3.3. Algorithm Design and Analysis

Based on the previous chapters, we design an algorithm (Algorithm 1) ED-HLOA for DenseNet201 to realize the self-adaptation of two hyperparameters.

Next, we verified its performance on a self-made dataset of Chinese medicinal materials.

4. Experimental Results and Analysis

4.1. General Setting

Evaluation Metrics. In practical applications, the accuracy of image classification is used to evaluate the performance of the model. This paper adopts three evaluation indicators, Precision-Recall and F_1 Score:

$$\text{Precision} = \frac{\text{TP}}{\text{TP} + \text{FP}} \quad (9)$$

$$\text{Recall} = \frac{\text{TP}}{\text{TP} + \text{FN}} \quad (10)$$

$$F_1 = 2 \times \frac{Precision \times Recall}{Precision + Recall} \quad (11)$$

where TP represents the number of true positives, which refers to the number of samples correctly predicted as positive by the model; FP represents the number of false positives, which refers to the number of samples incorrectly predicted as positive by the model; FN represents the number of false negatives, which refers to the number of positive samples incorrectly predicted as negative by the model. The higher the F_1 score, the better the performance of the model, representing a good balance between accuracy and recall.

Compare model. In this section, we compare the proposed ED-HLOA method with several state-of-the-art optimization algorithms, as well as with the default hyperparameters that have not undergone hyperparameter optimization, to validate its experimental performance. The methods of comparison are summarized as follows:

HLOA: HLOA is inspired by how horned lizard reptiles hide and protect themselves from predators [40];

PSO: Particle Swarm Optimization (PSO), which simulates the foraging behavior of bird flocks [38], is employed in this paper to optimize the hyperparameters of the CHM recognition model;

ESOA: Egret Swarm Optimization Algorithm (ESOA) to simulate egret predation and natural behavior [39];

WOA: Whale Swarm Algorithm (WOA), a heuristic optimization algorithm that simulates the behavior of whale predators [43];

CFOA: Fishing Optimization Algorithm (CFOA), inspired by traditional rural fishing methods [44];

F**A:** Firefly Algorithm (FA), inspired by the flashing behavior of fireflies [45];

Default: Based on the original DenseNet201 identification of the herbal medicine image recognition model, the default learning rate =0.001, compression factor =0.5.

To fairly evaluate the proposed method, for the CHM dataset, we use 80% of the images for the training set, 20% for the test set, and set aside 10% of the training set for the validation set. In this work, the TensorFlow framework is used to implement the proposed method, and all images are resized to 224 × 224 pixels as input. The batch size is set to 16, and stochastic gradient descent with a dynamic learning rate is used as the optimizer, continuing until the network converges. The experiments are conducted on a computer equipped with dual Intel Xeon E5-2620 v4 processors, two RTX A5000 GPUs, and 128 GB of RAM.

4.2. Performance Verification

In this section, we compare the performance of several algorithms in detail. Each algorithm conducts the same experiment five times, and not only chooses the best result among the five experiments for comparison, but also makes a comparative analysis of the average results of the five experiments. The two comparison results are shown in Table 2 and Table 3, and the curve diagrams of the training process are shown in Figs. 4-7. From these experimental results, we have the following findings:

Algorithm 1: ED-HLOA

Input: number of search agents D, population size P, maximum number of iterations T

Operation

/* Initialization */

Initialize D, P, T
Initialize: Population initialization

/* Training Starts */

for t=1 **to** $|T|$
  for i=1 **to** $|P|$
    if Crypsis? **Then**
      Strategy 1: Update x_i using Eq. (1).
    else
      if Flee? **Then**
        Strategy 4: Update x_i using Eq. (5).
      else
        Strategy 3: Update x_i using Eq. (4).
      end if
    end if
    Strategy 2: Replace the worst individual with Eq. (2) and Eq. (3).
    if melanophore(i) $\leqslant$ 0.3 **Then**
      Strategy 5: Generate a new position for x_i using Eq. (6) to replace it.
    end if
    Use Eq. (8) to obtain a new individual x_{new}.
    Update x_{best} using Eq. (9).
    end if
  end for
end for

/* Operation Ending */

Output: X_{best}, F_{best}

a) **The CHM identification model based on ED-HLOA achieves satisfactory accuracy and loss in both the training and testing sets.** We plot the corresponding accuracy and loss function curves based on the performance of different optimization algorithms in the experiments. The accuracy and loss function on the training set are shown in Figs. 4 and 5, respectively, while the accuracy and loss function on the validation set are shown in Figs. 6 and 7, respectively. The experimental results show that, on the training set, ED-HLOA consistently maintains a leading position throughout the training process, not only achieving a stable accuracy that surpasses other algorithms but also exhibiting a rapid decline in loss, demonstrating superior convergence. In terms of performance on the validation set, ED-HLOA slightly lags behind CFOA in the initial iterations, with lower accuracy and loss values, ranking second. However, as the iterations continue, the rate of decline in accuracy and loss for CFOA gradually slows down, while ED-HLOA demonstrates a stronger recovery capability, ultimately surpassing CFOA again and maintaining a stable leading advantage in subsequent iterations. It is evident that ED-HLOA's performance on the validation set not only reflects its exceptional convergence but also showcases its excellent generalization ability, achieving better predictive performance on unseen data.

Table 2 presents the best results of different optimization algorithms across five experiments. As shown in the table, ED-HLOA achieved an accuracy of 99.66% on the training set with a training loss of 0.0141, indicating its exceptional fitting ability during the training phase, as it attains high accuracy with minimal loss. Simultaneously, ED-HLOA also reached an accuracy of 99.16% on the test set, significantly outperforming other algorithms, with a test loss of only 0.0276, demonstrating its good generalization ability on unseen data.

In contrast, HLOA achieved a test set accuracy of 98.41% with a test loss of 0.0371. While its performance is close to that of ED-HLOA, it still falls short, particularly in high-precision tasks where slight differences can lead to significant performance discrepancies. Looking at the performance of other algorithms, the test set accuracies of ESOA, CFOA, and PSO decrease sequentially, recording values of 97.42%, 96.44%, and 96.33%, respectively, with corresponding test losses significantly increasing. Notably, the Default algorithm exhibited a test set accuracy of only 92.18% and a loss value as high as 0.2190, which is far below that of ED-HLOA, indicating poor performance with the default hyperparameter settings and insufficient optimization potential. This result underscores the importance of optimization algorithms based on fine-tuning of hyperparameters.

b) **In terms of precision, recall, and F1 score, ED-HLOA also performs the best.** As shown in Table 2, all three metrics achieve a value of 0.99, demonstrating its robustness and consistency in handling classification tasks. HLOA has values of 0.98 for all three metrics, which, while still excellent, are slightly inferior to those of ED-HLOA. The precision, recall, and F1 scores of other algorithms further decline, with CFOA and PSO recording values of 0.96, while Default only achieves 0.92, highlighting the comprehensive advantage of ED-HLOA across multiple metrics.

Overall, ED-HLOA's leading position in all metrics, particularly its performance on the test set, indicates that this algorithm not only converges quickly during training with low loss values but also possesses outstanding generalization ability. This result confirms the superiority of ED-HLOA in solving complex optimization problems, especially in tasks requiring high accuracy and low loss, where its performance significantly surpasses that of other optimization algorithms, reflecting its broad potential for practical applications.

c) **ED-HLOA ranks first in the average values of four key metrics: training set accuracy, training set loss, test set accuracy, and test set loss.** As shown in Table 3, a comparison is made between the various algorithms across five experiments, including their metrics and standard deviations. The experimental results indicate that the average test set accuracy of ED-HLOA reached 98.59%, significantly outperforming other algorithms; its average test set loss was only 0.0382, demonstrating the model's good fitting performance on the test data. Furthermore, ED-HLOA's performance in terms of test set accuracy is particularly outstanding, showing an improvement of 0.94% compared to the second-ranked HLOA algorithm, further proving the advantages of ED-HLOA in handling practical tasks.

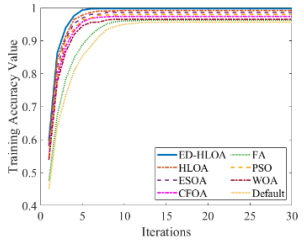

Figure 4. Training set accuracy results

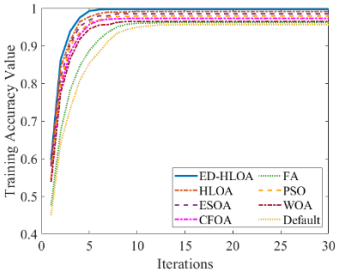

Figure 5. Loss results of training set

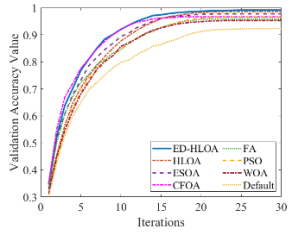

Figure 6. Validation set accuracy results

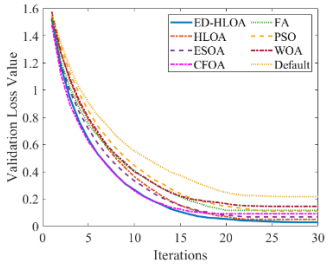

Figure 7. Loss results of validation set

Table 2.Comparison of the Best Results From Five Experiments

Baseline	TrainingAccuracy	TrainingLoss	TestAccuracy	TestLoss	Precision	Recall	F1-score
HLOA	0.9908	0.0248	0.9841	0.0371	0.98	0.98	0.98
ESOA	0.9850	0.0325	0.9742	0.0696	0.97	0.97	0.97
CFOA	0.9827	0.0605	0.9644	0.1027	0.96	0.96	0.96
FA	0.9768	0.0715	0.9540	0.1208	0.95	0.95	0.95
PSO	0.9838	0.0565	0.9633	0.1164	0.96	0.96	0.96
WOA	0.9793	0.0701	0.9512	0.1421	0.95	0.95	0.95
Default	0.97086	0.0911	0.9218	0.2190	0.92	0.92	0.92
ED-HLOA	**0.9965**	**0.0141**	**0.9916**	**0.0276**	**0.99**	**0.99**	**0.99**

Table 3. Comparison of the Average Values (±std) of All Algorithms

Baseline	TrainingAccuracy	TrainingLoss	TestAccuracy	TestLoss
HLOA	0.9864±0.004005	0.0432±0.016985	0.9765±0.008786	0.0648±0.027992
ESOA	0.9808±0.003733	0.0607±0.016805	0.9687±0.004765	0.0891±0.024720
CFOA	0.9789±0.003883	0.0680±0.006255	0.9559±0.007157	0.1294±0.020330
FA	0.9739±0.002982	0.0796±0.014611	0.9480±0.005451	0.1483±0.019603
PSO	0.9812±0.002833	0.0621±0.006192	0.9566±0.006245	0.1260±0.015188
WOA	0.9762±0.003103	0.0751±0.004857	0.9466±0.003992	0.1531±0.008017
Default	0.9693±0.000965	0.1016±0.0072	0.9174±0.002629	0.2280±0.005830
ED-HLOA	**0.9935**±0.002758	**0.0171**±0.003609	**0.9859**±0.004396	**0.0382**±0.009403

In the comparison of standard deviations, the Default (default hyperparameter settings) shows relatively small standard deviations across all metrics. In contrast, ED-HLOA ranks second in terms of training set standard deviation, indicating that its fluctuations on the training set are relatively minor, maintaining a certain level of stability. On the test set, ED-HLOA ranks third in standard deviation; although there are slight fluctuations, its average performance still surpasses that of other algorithms.

Overall, ED-HLOA demonstrates excellent performance across multiple metrics, particularly excelling in the comprehensive evaluation of accuracy and loss values, showcasing good optimization capability and generalization performance. While it exhibits slight shortcomings in stability, its overall performance remains at a high level, sufficiently demonstrating the robustness and adaptability of ED-HLOA in complex problems.

d) **ED-HLOA demonstrates excellent convergence on both the training set and validation set.** As shown in Figs. 8 and 9, after 100 iterations, ED-HLOA exhibits outstanding convergence on both datasets. Notably, the convergence speed of the algorithm on the training set is particularly remarkable, with convergence achieved in approximately 20 iterations. Furthermore, throughout the subsequent iterations, the accuracy of the training set nearly approaches 1, indicating that the model has reached an optimal fitting state.

To verify robustness, we conducted five independent runs. The average training accuracy was 0.9985 (std: 0.00030), and training loss averaged 0.00185 (std: 0.00005). On the validation set, the mean accuracy was 0.9911 (std: 0.00048), and loss was 0.03006 (std: 0.00087). These results confirm the model's stable performance across runs.

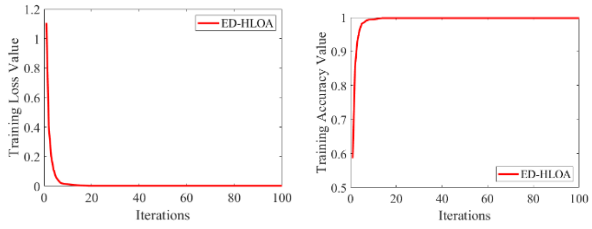

(a) Accuracy (b) Loss

Figure 8. Accuracy and Loss results of training set

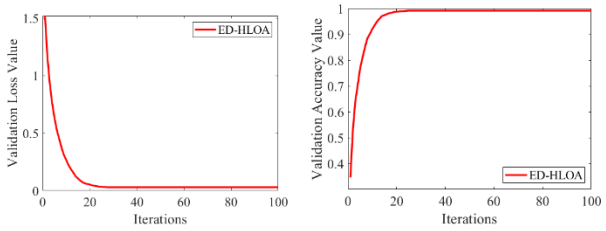

(a) Accuracy (b) Loss

Figure 9. Accuracy and Loss results of validation set

5. Conclusions

This study proposed the Elite Differential Mutation-based Horned Lizard Optimization Algorithm (ED-HLOA) to optimize the learning rate and compression factor of the DenseNet201 model, which was validated on a self-constructed herbal medicine image dataset. The experimental results indicate that ED-HLOA significantly enhances the classification performance of DenseNet201, with notable improvements in accuracy and loss values on both the training and validation sets. Furthermore, it demonstrates rapid convergence characteristics in optimizing the learning rate and compression factor, thereby improving training efficiency. The DenseNet201 model optimized by ED-HLOA achieved high accuracy in the classification tasks of herbal medicine images, validating the algorithm's effectiveness in practical applications.

Compared to several state-of-the-art optimization algorithms, ED-HLOA excels in both the training and validation sets, avoiding overfitting and demonstrating high efficiency, robustness, and generalization capability. Notably, the potential of CHM in tumor treatment has been validated by extensive research. Therefore, the study on high-precision recognition of CHM images not only carries classificatory significance but also provides a fundamental basis for subsequent investigations into the anti-tumor mechanisms of Chinese medicine, efficacy screening, and the construction of intelligent auxiliary diagnosis and treatment systems. Future research could expand the application scope of ED-HLOA, enrich the herbal medicine dataset to include a broader range of medicinal materials, and incorporate the latest image classification models to further enhance recognition accuracy for different states of herbal medicines (such as raw herbs, slices, etc.). Furthermore, the deep integration of image recognition technology with pharmacological databases can be employed to explore the potential correlations between the image features of specific medicinal materials and their anti-tumor active components, providing technical support for the intelligent screening of CHM-assisted tumor therapy and the formulation of personalized medication plans.

Acknowledgements

This research is supported by the Chengdu University of Information Technology key project of education reform (JYJG2024206) and the Key Laboratory of Remote Sensing Application and Innovation (LRSAI-2025004).

References

[1] Xing D, Liu Z. Effectiveness and Safety of Traditional Chinese Medicine in Treating COVID-19: Clinical Evidence from China. Aging and Disease. 2021. Dec 1;12(8):1850-1856.

[2] Lu AP, Jia HW, Xiao C, Lu QP. Theory of traditional Chinese medicine and therapeutic method of diseases. World J Gastroenterol. 2004 Jul 1;10(13):1854-6.

[3] Gu J, Zhang J, Zeng S, et al. Artificial intelligence in tumor drug resistance: Mechanisms and treatment prospects. Intelligent Oncology. 2025;1: 73-78.

[4] Ye X, Guo D, Zhao L, et al. Development and validation of AI delineation of the thoracic RTOG organs at risk with deep learning on multi-institutional datasets. Intelligent Oncology. 2025; 1: 61-71.

[5] Wu N, Wu G, Hu R, et al. Ginsenoside Rh2 inhibits glioma cell proliferation by targeting microRNA-128[J]. Acta Pharmacologica Sinica, 2011, 32(3): 345-353.

[6] Tan X, Ma X, Dai Y, et al. A large-scale transcriptional analysis reveals herb-derived ginsenoside F2 suppressing hepatocellular carcinoma via inhibiting STAT3[J]. Phytomedicine, 2023, 120: 155031.

[7] Li Z, Feiyue Z, Gaofeng L. Traditional Chinese medicine and lung cancer — — From theory to practice[J]. Biomedicine & Pharmacotherapy, 2021, 137: 111381.

[8] Wang S, Fu J L, Hao H F, et al. Metabolic reprogramming by traditional Chinese medicine and its role in effective cancer therapy[J]. Pharmacological research, 2021, 170: 105728.

[9] Jeny F, Nunes H. Le granulome sarcoïdien [Sarcoidosis granuloma]. Rev Prat. 2016 Feb;66(2):e47-e48. French. PMID: 30512345.

[10] N. Beulah Jabaseeli, D. Umanandhini, Medicinal plant species detection by comparison review, Journal of the Saudi Society of Agricultural Sciences, 2024, ISSN 1658-077X.

[11] J. Li, S. Wang, J. Zhang, M. Feng, Y. Zhu and S. Wu, "Research and Discussion on Chinese Traditional Medicine Health Culture Literacy——Based on Visual Analysis of CiteSpace," 2021 International Conference on Health Big Data and Smart Sports (HBDSS), Guilin, China, 2021, pp. 34-38.

[12] Q. Zhang, F. Yang and Y. Liu, "Evolution of Research Themes in Traditional Chinese Medicine in China-Reflections on Advancing Internationalization of Traditional Chinese Medicine Research," 2023 7th Asian Conference on Artificial Intelligence Technology (ACAIT), Jiaxing, China, 2023, pp. 577-584.

[13] L. Wu, Y. Wang, J. Jiang and C. Guo, "Research on the application of an improved deep convolutional neural network in image recognition," 2020 International Conference on Virtual Reality and Intelligent Systems (ICVRIS), Zhangjiajie, China, 2020, pp. 470-472.

[14] S. Marinai, M. Gori and G. Soda, "Artificial neural networks for document analysis and recognition," in IEEE Transactions on Pattern Analysis and Machine Intelligence, vol. 27, no. 1, pp. 23-35, Jan. 2005.

[15] Y. Zhang and W. Ge, "AUV Path Planning and Image Recognition Based on Convolutional Neural Network," 2022 3rd International Conference on Big Data, Artificial Intelligence and Internet of Things Engineering (ICBAIE), Xi'an, China, 2022, pp. 605-608.

[16] R. Zhao, Y. Wang, P. Jia, C. Li, Y. Ma and Z. Zhang, "Abnormal Human Behavior Recognition Based on Image Processing Technology," 2021 IEEE 5th Advanced Information Technology, Electronic and Automation Control Conference (IAEAC), Chongqing, China, 2021, pp. 1924-1928.

[17] H. Jeong, J. Shin, F. Rameau and D. Kum, "Multi-Modal Place Recognition via Vectorized HD Maps and Images Fusion for Autonomous Driving," in IEEE Robotics and Automation Letters, vol. 9, no. 5, pp. 4710-4717, May 2024.

[18] F. Xu, F. Xu, J. Xie, C. -M. Pun, H. Lu and H. Gao, "Action Recognition Framework in Traffic Scene for Autonomous Driving System," in IEEE Transactions on Intelligent Transportation Systems, vol. 23, no. 11, pp. 22301-22311, Nov. 2022.

[19] L. Zhou, L. Zhang and N. Konz, "Computer Vision Techniques in Manufacturing," in IEEE Transactions on Systems, Man, and Cybernetics: Systems, vol. 53, no. 1, pp. 105-117, Jan. 2023.

[20] X. Zhou et al., "Automated Estimation of the Upper Surface of the Diaphragm in 3-D CT Images," in IEEE Transactions on Biomedical Engineering, vol. 55, no. 1, pp. 351-353, Jan. 2008, doi: 10.1109/TBME.2007.899337.

[21] J. Li, Z. Yang and Y. Yu, "A Medical AI Diagnosis Platform Based on Vision Transformer for Coronavirus," 2021 IEEE International Conference on Computer Science, Electronic Information Engineering and Intelligent Control Technology (CEI), Fuzhou, China, 2021, pp. 246-252.

[22] Peiyang W, Hongping S, Jianhong G, et al. Sequential Recommendation System Based on Deep Learning: A Survey[J]. Electronics, 2025, 14(11): 2134.

[23] Wen Z, Lan H, Khan M A. Apple disease detection and classification using Random Forest (One-vs-All). AIRO. 2025;:8041.

[24] Dwivedi A, Khan A T, Li S. Comparative Analysis of BAS and PSO in Image Transformation Optimization[J]. 2025.

[25] He, Kaiming, et al. "Deep residual learning for image recognition." Proceedings of the IEEE conference on computer vision and pattern recognition. 2016.

[26] Szegedy C, Liu W, Jia Y, et al. Going deeper with convolutions[C]//Proceedings of the IEEE conference on computer vision and pattern recognition. 2015: 1-9.

[27] Huang, Gao, et al. "Densely connected convolutional networks." Proceedings of the IEEE conference on computer vision and pattern recognition. 2017.

[28] Chen L, Jin L, Shang M, et al. Enhancing representation power of deep neural networks with negligible parameter growth for industrial applications[J]. IEEE Transactions on Systems, Man, and Cybernetics: Systems, 2024.

[29] H. Ji, X. Liu, L. Wang, L. Fan and S. Liu, "Image Recognition of Chinese Herbal Medicine Using Adaptive Gamma Correction Based on Convolutional Neural Network," 2024 IEEE 13th Data Driven Control and Learning Systems Conference (DDCLS), Kaifeng, China, 2024, pp. 1428-1433.

[30] S. M. Kadiwal, V. Hegde, N. Shrivathsa, S. Gowrishankar, A. H. Srinivasa and A. Veena, "Deep Learning based Recognition of the Indian Medicinal Plant Species," 2022 4th International Conference on Inventive Research in Computing Applications (ICIRCA), Coimbatore, India, 2022, pp. 762-767.

[31] Chen Z, Li S, Khan A T, et al. Competition of tribes and cooperation of members algorithm: An evolutionary computation approach for model free optimization[J]. Expert Systems with Applications, 2025, 265: 125908.

[32] Wei P, Hu C, Hu J, et al. A Novel Black Widow Optimization Algorithm Based on Lagrange Interpolation Operator for ResNet18[J]. Biomimetics, 2025, 10(6): 361.

[33] Wei P, Shang M, Zhou J, et al. Efficient adaptive learning rate for convolutional neural network based on quadratic interpolation egret swarm optimization algorithm[J]. Heliyon, 2024, 10(18).
[34] X. Luo, J. Chen, Y. Yuan and Z. Wang, "Pseudo Gradient-Adjusted Particle Swarm Optimization for Accurate Adaptive Latent Factor Analysis," in IEEE Transactions on Systems, Man, and Cybernetics: Systems, vol. 54, no. 4, pp. 2213-2226.
[35] J. Chen et al., "A State-Migration Particle Swarm Optimizer for Adaptive Latent Factor Analysis of High-Dimensional and Incomplete Data," in IEEE/CAA Journal of Automatica Sinica, vol. 11, no. 11, pp. 2220-2235, November 2024.
[36] A. Bajaj and O. P. Sangwan, "A Systematic Literature Review of Test Case Prioritization Using Genetic Algorithms," in IEEE Access, vol. 7, pp. 126355-126375, 2019.
[37] A. Ebrahimi and A. Rahimian, "Estimation of channel parameters in a multipath environment via optimizing highly oscillatory error functions using a genetic algorithm," 2007 15th International Conference on Software, Telecommunications and Computer Networks, Split, Croatia, 2007, pp. 1-5.
[38] Dianwei Wang, Leilei Zhai, Jie Fang, Yuanqing Li, Zhijie Xu, “psoResNet: An improved PSO-based residual network search algorithm,” Neural Networks, Volume 172, 2024.
[39] Kong, Zhengyi, et al. "Hybrid machine learning with optimization algorithm and resampling methods for patch load resistance prediction of unstiffened and stiffened plate girders." Expert Systems with Applications 249 (2024): 123806.
[40] Peraza-Vázquez, H., Peña-Delgado, A., Merino-Treviño, M. et al. A novel metaheuristic inspired by horned lizard defense tactics. Artif Intell Rev 57, 59 (2024).
[41] Gu Q, Li S, Liao Z. Solving nonlinear equation systems based on evolutionary multitasking with neighborhood-based speciation differential evolution. Expert Systems with Applications. 2024; 238: 122025.
[42] Sun J, Gao S, Dai H, et al. Bi-objective elite differential evolution algorithm for multivalued logic networks. IEEE Transactions on Cybernetics. 2018; 50(1): 233-246.
[43] Sapnken, Flavian Emmanuel, et al. A whale optimization algorithm-based multivariate exponential smoothing grey-holt model for electricity price forecasting. Expert Systems with Applications. 2024;255: 124663.
[44] Jia, Heming, et al. Catch fish optimization algorithm: a new human behavior algorithm for solving clustering problems. Cluster Computing. 2024; 1-38.
[45] Yang B, Zhang Z, Zhang J, et al. Optimal reconfiguration design and HIL validation of hybrid PV-TEG systems via improved firefly algorithm. Energy. 2024;286: 129648.

Data availability

Data and Codes that support the findings of this study have been deposited in the GitHub with the link https://github.com/aliwa8168/ED-HLOA

Author Contributions

Peiyang Wei. Rundong Zou: Conceptualization, Methodology, Software,Writing- Reviewing and Editing. Wen Qin. Jianhong Gan: Data curation, Writing- Original draft preparation. Peiyang Wei. Rundong Zou. Guangtong Dong: Visualization, Investigation. Xun deng. Qifeng Su. Zhibin Li:Supervision,Software, Validation. All authors reviewed the manuscript.

Competing Interests

No, I declare that the authors have no competing interests as defined by Nature Research, or other interests that might be perceived to influence the results and/or discussion reported in this paper.